Adv-watermark: A Novel Watermark Perturbation for Adversarial Examples

Xiaojun Jia
jiaxiaojun@iie.ac.cn
Institute of Information Engineering, Chinese Academy of Sciences
Beijing, China

Xingxing Wei*
xxwei@buaa.edu.cn
Beijing Key Laboratory of Digital Media, School of Computer Science and Engineering, Beihang University
Beijing, China

Xiaochun Cao*
caoxiaochun@iie.ac.cn
Institute of Information Engineering, Chinese Academy of Sciences
Beijing, China

Xiaoguang Han
hanxiaoguang@cuhk.edu.cn
Shenzhen Research Institute of Big Data, the Chinese University of Hong Kong (Shenzhen)
Shenzhen, Guangdong, China

ABSTRACT

Recent research has demonstrated that adding some imperceptible perturbations to original images can fool deep learning models. However, the current adversarial perturbations are usually shown in the form of noises, and thus have no practical meaning. Image watermark is a technique widely used for copyright protection. We can regard image watermark as a king of meaningful noises and adding it to the original image will not affect people's understanding of the image content, and will not arouse people's suspicion. Therefore, it will be interesting to generate adversarial examples using watermarks. In this paper, we propose a novel watermark perturbation for adversarial examples (Adv-watermark) which combines image watermarking techniques and adversarial example algorithms. Adding a meaningful watermark to the clean images can attack the DNN models. Specifically, we propose a novel optimization algorithm, which is called Basin Hopping Evolution (BHE), to generate adversarial watermarks in the black-box attack mode. Thanks to the BHE, Adv-watermark only requires a few queries from the threat models to finish the attacks. A series of experiments conducted on ImageNet and CASIA-WebFace datasets show that the proposed method can efficiently generate adversarial examples, and outperforms the state-of-the-art attack methods. Moreover, Adv-watermark is more robust against image transformation defense methods.

CCS CONCEPTS

• **Computing methodologies** → Image recognition and understanding.

*Corresponding Author

KEYWORDS

Adversarial Examples, Watermark Perturbation, Basin Hopping Evolution

ACM Reference Format:
Xiaojun Jia, Xingxing Wei, Xiaochun Cao, and Xiaoguang Han. 2020. Adv-watermark: A Novel Watermark Perturbation for Adversarial Examples. In *Proceedings of the 28th ACM International Conference on Multimedia (MM '20), 12-16 October 2020 Seattle, United States.* ACM, New York, NY, USA, 10 pages. https://doi.org/10.1145/1122445.1122456

1 INTRODUCTION

Recent literature has found that Deep Neural Networks (DNNs) are vulnerable to the adversarial examples which are generated by adding some imperceptible noises to the clean images [5]. Generally speaking, attack methods can be divided into two categories: white-box attack methods and black-box attack methods. The white-box attack [2, 6, 15, 23] denotes that the attacker has complete access to the target model such as model parameters, model structure, etc. And the black-box attack [1, 4, 29, 33] denotes that the attacker can only access the output of the target model. The above methods achieve attacks by generating imperceptible perturbations. They use L_0, L_2, L_∞ to bound the noises. Recently, more and more researchers pay attention to generating realistic adversarial examples without the L_p norm limitation. For example, a semantic-based perturbation (SemanticAdv) is proposed in [26]. It generates an unrestricted adversarial example by manipulating the semantic attributes of images. In [16], Lagae et al. propose to generate adversarial examples by using procedural noise functions which are widely used in computer graphics. And in [4], Engstrom et al. use the chosen rotations and translations to generate the adversarial examples. Compared with the adversarial examples under L_p norm constraint, the unrestricted adversarial examples are more realistic and practical. Following up the unrestricted attack methods, we propose a novel attack method which uses the meaningful perturbations to generate adversarial examples in this paper.

Watermarking methods [7] play an important role in protecting intellectual property rights. It embeds some specific information of the copyright holder (such as university logos, ownership descriptions, etc) into the multimedia data according to the requirements of

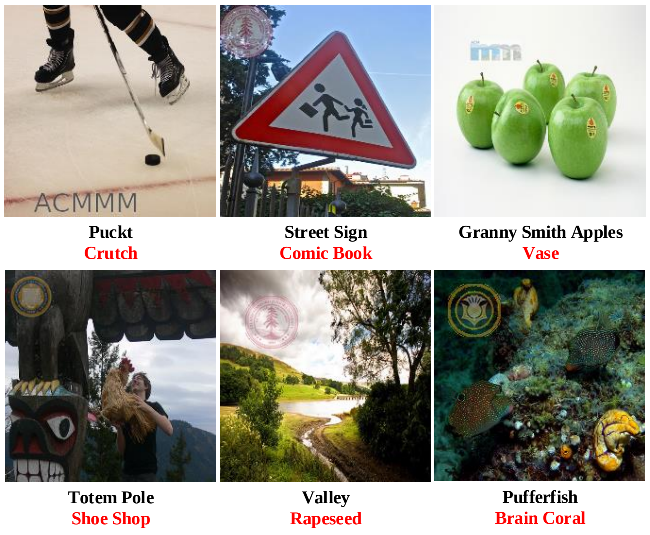

Figure 1: Adversarial examples with watermark perturbations. The original class labels are in black text and the adversarial class labels are in red text.

users. With the digital libraries, the research of visible watermark is becoming more and more important. In [20], Mintzer et al. describe the characteristics of visible watermarks. The visible watermark should be visible but does not significantly obscure the details of the host image. In [21], the IBM digital library organization proposes to use a visible watermark to mark the digitized pages of the Vatican archive manuscript.

In this paper, we propose a novel adversarial attack which generates adversarial examples using watermarks. We find that although watermarks do not affect people's understanding of the image content, and adding specific watermarks to the clean images can fool the DNN models. The specific watermarks refer to the specific position and transparency of them. We mainly consider using visible watermarks to generate adversarial examples. In detail, we use alpha blending [31] to achieve watermark embedding. The host image and the watermark are multiplied by a scaling factor. The scaling factor is manipulated in the α channel of the image, which decides the image's transparency.

As for a certain watermark, the DNN models can be successfully attacked only by adding the watermark with the specific transparency to a specific position of the host image. Considering this, we propose a novel attack method to generate watermark adversarial perturbations based on the optimization algorithms. Specifically, we propose a Basin Hopping Evolution (BHE) algorithm to find the appropriate transparency of the watermark image and the appropriate position within the host image to embed watermark. BHE is proposed based on the Hopping Evolution (BH) [36], where we find it usually falls into a local optimum and fails in attacking DNN models. In contrast, BHE has multiple initial starting points and crossover operation to keep the diversity of solutions. In this way, BHE makes it easier to find a global optimal solution and thus achieves a higher attack success rate than BH. The proposed method achieves attacks by using a little information (predicted probability of the classification model). It does not need the inner information of DNNs such as

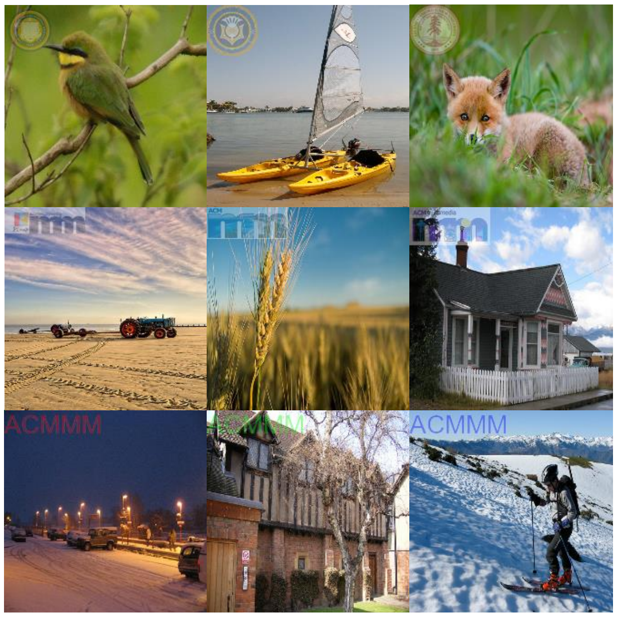

Figure 2: In this paper, we explore two kinds of media as the watermark: logos and texts. The top row uses university logo watermarks. The middle row uses the official logo of ACMMM. The bottom row is text watermarks of ACMMM with different colors. These nine host images are randomly selected from ImageNet.

network structures and weights, and can attack many types of DNNs even if the gradient of the network is difficult to calculate. Therefore, it belongs to the black-box attack.

Besides the ability to perform adversarial attacks, Adv-watermark also inherits the function of the visible watermark. That's to say, Adv-watermark can also protect the copyright of the image because it carries the owner's description. Therefore, Adv-watermark can accomplish two functions at the same time. This is a major advantage compared with the previous research. In this paper, we explore two kinds of media as the watermarks: logos and texts. Figure 2 lists the used watermarks, and some generated Adv-watermark examples are shown in Figure 1.

In summary, this paper has the following contributions:

1) We propose the Adv-watermark, a novel watermark perturbation for adversarial examples, which combines image watermarking techniques and adversarial example algorithms. Compared with the previous works, the proposed adversarial example is more realistic and effective. The Adv-watermark has the watermark characteristic (copyright protection) and adversarial example function (fool the well-trained classifier) at the same time.

2) We propose a novel optimization algorithm, which is called Basin Hopping Evolution (BHE), to generate adversarial examples efficiently. The proposed method adopts a population-based global search strategy to generate adversarial examples, and can achieve high performance in attacking DNN models.

3) Compared with the previous black-box attack methods, the proposed method can achieve a higher attack success rate. In detail, it can achieve an above 97% black-box attack success rate when the

watermark size is 4/9 of the host image size. Even if the watermark size is 1/16 of the host image size, it also can achieve an about 65% attack success rate. Moreover, it is difficult to defend the proposed attack method using the state-of-the-art image transformation defense methods.

The remainder of this paper is organized as follows. Section 2 briefly reviews the related work. Section 3 introduces the details of the proposed Adv-watermark. Section 4 shows a series of experimental results and analysis. Finally, Section 5 gives the conclusion.

2 RELATED WORK

In this section, we investigate the attack methods and the visible watermarking methods.

2.1 Attack methods

In [6], Goodfellow et al. devise an effective method to calculate the adversarial examples, and the adversarial perturbation is generated according to the direction of the gradient change of the DNNs. This method is also called FGSM. Iterative FGSM (I-FGSM) [15] is an improved version of FGSM. I-FGSM constructs an adversarial example by multi-step and smaller movements, which greatly improves the success rate of the attack. The most common adversarial attack methods are under the L_∞ and L_2 distance metric. But in [24], Papernot et al. propose to build adversarial saliency maps to generate adversarial examples under L_0 norm. Moosavi-Dezfooli et al. propose a simple and accurate method (Deepfool) [23] to efficiently generate the adversarial examples. Moreover, they further propose the universal perturbation based on Deepfool in [22]. And in [2], Carlini and Wagner propose three attack methods to attack defensive distillation Networks [25]. In [33], Su at el. propose to generate one-pixel adversarial perturbations based on differential evolution (DE). That is, only one pixel can be changed to generate an adversarial example, which is an extreme attack method.

2.2 Visible watermarking methods

In [13], Kankanhalli et al. propose a visible watermarking technique that can find the strength of the watermark image and the location of the host image to embed watermark automatically in the DCT domain. In [31], Shen et al. propose to use the alpha blending technique to generate the visible watermark. A removable visible watermark is proposed in [9]. They design a vision watermarking algorithm suitable for the different requirements of the applications. In [18], Liu et at. propose a new approach to generate a generic lossless visible watermark. The proposed method makes use of deterministic one-to-one mappings of image pixel values to achieve generating the visible watermark. In [10], Huang et al. design a visible watermarking algorithm for digital right management. A contrast-sensitive function and block classification are used to achieve a better visual effect in the discrete wavelet transform domain.

3 METHODOLOGY

In this section, we introduce the proposed method from three aspects: visible watermarking, problem formulation and problem solving.

3.1 Visible Watermarking

We use alpha blending in [31] to generate a visible watermark. Alpha channel(α channel) refers to the transparency of a foreground region w.r.t. the background image. In this paper, we use α to represent the value of the alpha channel, H to represent the host image whose size is $N \times M$, W to represent the watermark image whose size is $n \times m$ and G to represent the generated image with a watermark whose size is $N \times M$. When $i \in (p, p+n), j \in (q, q+m)$, the generation for G is formulated as:

$$v(G)_{i,j} = (v(W)_{i-p,j-q} * \alpha + v(H)_{i,j} * (255 - \alpha))/255 \quad (1)$$

when $i \notin (p, p+n), j \notin (q, q+m)$, G is formulated as:

$$v(G)_{i,j} = v(H)_{i,j}, \quad (2)$$

where $v(x)$ denotes the image x, the subscript i, j of $v(x)$ represent the pixel position, and p, q represent the position where the watermark image is embedded. In this paper, we not only use the image watermark, but also use the text watermark. We first convert the text into an image and then process it. As for the image watermark, we use UC Berkeley, CMU, MIT, Cambridge and Stanford University logo watermarks. Simultaneously, we also use the official ACMMM logo from 2016 to 2020. As for text watermark, we use red, green, blue, black and gray fonts to generate adversarial examples. We also synthesize watermark images in different sizes to explore scale-ware effects. It is formulated as:

$$\begin{aligned} &\eta = \min((W_h * sl)/W_w, (H_h * sl)/H_w), \\ &W_{sw} = W_w * \eta, H_{sw} = H_w * \eta, \end{aligned} \quad (3)$$

where W_h and H_h represent the width and height of the host image. W_w and H_w represent the width and height of the watermark image. sl is the scaling factor. And W_{sw} and H_{sw} represent the width and height of the scaled watermark image. Note that in this paper, we focus on the position and transparency of the watermark, not the rotation, etc.

3.2 Problem Formulation

We disguise adversarial noise as a visible watermark to achieve stealthiness. And the generation of adversarial examples is only related to the position and transparency of the watermark. Generating adversarial watermark images can be formalized as an optimization problem with constraints. The host image is assumed as H, the well-trained classification model is assumed as f and the correct classification class of H is t. $f_t(H)$ is the probability of H belonging to the class t. Simultaneously, let W be the watermark image and $g(H, W, p, q, \alpha)$ be the visible watermark algorithm. It embeds the watermark image W in the position (p, q) of the host image H. The p, q and α are dependent on W, H, f. And the limitation of maximum transparency of the watermark is L. In the case of untargeted attacks, the goal of generation of adversarial examples can be transformed into finding the optimized solution $e(p, q, \alpha)^*$. It is formulated as:

$$\begin{aligned} \underset{e(p,q,\alpha)^*}{\text{minimize}} \quad & f_t(g(H, W, p, q, \alpha)) \\ \text{subject to} \quad & \alpha \le L \end{aligned} \quad (4)$$

This problem involves two values: 1) the position (p, q) of the watermark in the host image and 2) the transparency α of the watermark. Embedding the adversarial watermark which can be regarded as a practical perturbation into the host image modifies the local

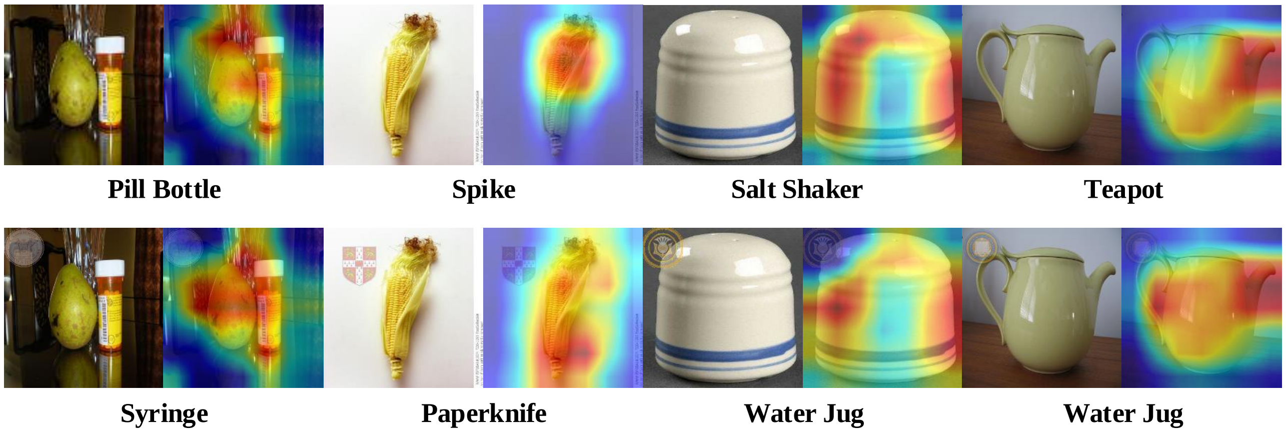

Figure 3: The top row is the original images (they are correctly classified by Resnet101) and their corresponding heat-maps (generated by Grad-CAM algorithm).The bottom row is the adversarial images with the visible watermark and their corresponding heat-maps. The image classification labels are in black color.

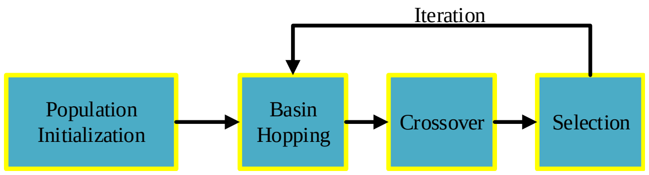

Figure 4: The process of Basin Hopping Evolution.

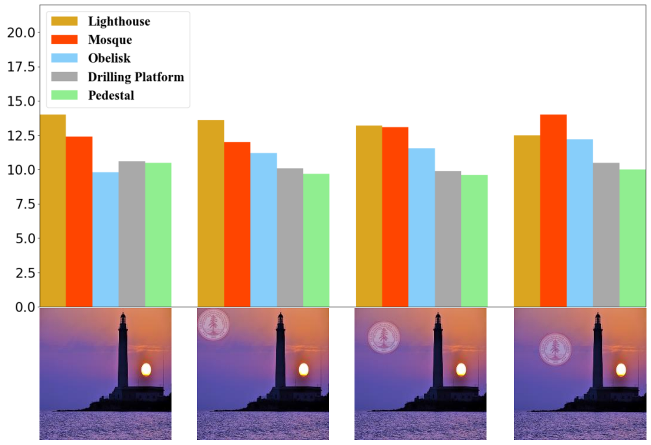

Figure 5: The histogram of the top 5 category confidence of generated images in the generation process of the adversarial examples using BHE.

information of the host image. In this way, the adversarial watermark perturbation permits a clean image to be an adversarial example. Without affecting the visual effect of the image, the adversarial watermark disturbs the important local regions which determine the image classification to attack the well-trained classification model. This is illustrated in Figure 3. From the heat-maps which are generated by Gradient-weighted Class Activation Mapping (Grad-CAM) [30], it is clear why the Resnet101 predicts the input images as the corresponding correct classes. And embedding the adversarial watermark into the image can modify the distribution of the maximum points on the generated heat-map.

3.3 Problem Solving

We propose a novel optimization algorithm, which is called Basin Hopping Evolution(BHE). The proposed method is a heuristic random search algorithm based on Basin Hopping, which can be used for finding the global minimum of a multivariate function. As shown in Figure 4, BHE includes Basin Hopping, crossover and selection operations. During each iteration, the current solutions (parents) use BH to produce a set of better solutions and conduct crossover operation to generate a new set of candidate solutions (children). And then in selection operation, compared with the corresponding parents to conduct, if the children are more suitable for the current population evolution (posses the smaller multivariate function value), they survive and are passed to the next generation.

3.3.1 Population Initialization. BHE is an optimization algorithm based on group evolution. We regard each solution as an individual of a population. And the elements (p, q and α) are considered as its genes. Let $X_{i,g}$ denote the i-th individual in the g-th generation population. And $X_{i,g,j}(j = 0, 1, 2)$ denotes the j-th gene of $X_{i,g}$. Therefore, we initialize a population as follows:

$$X_{i,0,j} = X_{\min,j} + rand(0,1) \cdot (X_{\max,j} - X_{\min,j}), j = 0, 1, 2 \quad (5)$$

where $X_{i,0,j}$ is the j-th gene of the i-th individual in the initial population , $X_{\min,j}$ is the minimum of the j-th gene and $X_{\max,j}$ is the maximum of the j-th gene.

3.3.2 Basin Hopping. Basin Hopping (BH) is a stochastic optimization algorithm. During each iteration, BH generates some new coordinates with random perturbations, next finds the local minimization, and finally accepts or rejects the new coordinates according to the minimized function value. We use BH to evolve a better individual $V_{i,g}$ from $X_{i,g}$.

In detail, $f_t(g(H, W, p, q, \alpha))$ is assumed as $f_t(\cdot)$. Starting with $X_{i,g}$, a local optimal solution $V_{i,g}$ of the function $f_t(\cdot)$ is found by using a minimization method $L(\cdot)$. Next we start the global search iterations and use $\mu_g(X_{i,g})$ to represent the global neighborhood of $X_{i,g}$. It is formulated as:

$$\mu_g(X_{i,g}) = [X_{i,g}, X_{i,g} + r * \vec{d}], \tag{6}$$

where $\vec{d}$ is an n-dimensional Gaussian$(0, 1)$ variable and r is a fixed step size. A new starting point is selected from the global neighborhood of $V_{i,g}$. It is stored as $V_{i,g}$.It is formulated as:

$$V_{i,g} = G(\mu_g(V_{i,g})) \tag{7}$$

And then starting with $V_{i,g}$, a local search is performed and the result is stored as $S_{i,g}$. Finally, we use a function $Accept(V_{i,g}, S_{i,g})$ to choose $V_{i,g}$ or $S_{i,g}$. And it is formulated as:

$$Accept(V_{i,g}, S_{i,g}) = \begin{cases} 1 & f_t(S_{i,g}) \le f_t(V_{i,g}) \\ 0 & f_t(S_{i,g}) > f_t(V_{i,g}) \end{cases} \tag{8}$$

The detail description is given in Algorithm 1. To represent BH algorithm simplify, it can be formulated as:

$$V_{i,g} = BH(X_{i,g}, I), \tag{9}$$

where $X_{i,g}$ represents the i-th solution in the g-th generation population, $V_{i,g}$ represents the corresponding better solution using BH, $BH(\cdot)$ represents the BH algorithm and I indicates the maximum number of Basin Hopping iterations which is a super parameter which we use a large number of experiments to certify.

Algorithm 1 BH algorithm

```
Require: The watermark image $W$, the host image $H$, the well-trained classifier $f$ and $X_{i,g}$
Ensure: $V_{i,g}$
1: $V_{i,g} = L(f_t(\cdot), X_{i,g})$;
2: repeat
3:     $V_{i,g} = G(\mu_g(V_{i,g}))$;
4:     $S_{i,g} = L(f_t(\cdot), V_{i,g})$;
5:     if $Accept(V_{i,g}, S_{i,g})$ then
6:         $V_{i,g} = S_{i,g}$;
7:     end if
8: until global stopping rule is satisfied
9: return $V_{i,g}$
```

3.3.3 Crossover. As for the current solution (parents) $X_{i,g}$ and the corresponding BH optimization solution $V_{i,g}$, we conduct crossover operation to get a candidate solution (child) $U_{i,g}$. It is formulated as:

$$U_{i,g,j} = \begin{cases} V_{i,g,j}, rand(0,1) \le \text{CR} \\ X_{i,g,j}, \text{ others} \end{cases} \tag{10}$$

where $U_{i,g,j}$ is the j-th gene of $U_{i,g}$, $V_{i,g,j}$ is the j-th gene of $V_{i,g}$, $X_{i,g,j}$ is the j-th gene of $X_{i,g}$ and CR is the crossover probability which represents the degree of information exchange in the population evolution. It is a super parameter which we use a large number of experiments to certify.

3.3.4 Selection. We adopt a greedy selection strategy to select a better solution as the next generation solution. It is formulated as:

$$X_{i,g+1} = \begin{cases} \text{U}_{i,g}, f_t\left(U_{i,g}\right) \le f_t\left(X_{i,g}\right) \\ X_{i,g} \text{ others} \end{cases} \tag{11}$$

The detail description of BHE is given in Algorithm 2. And the generation process of the adversarial examples by using BHE is shown in Figure 5.

Algorithm 2 BHE algorithm

```
Require: Population: $M$; Dimension: 3; Generation: $N$; Iteration: $I$;
Ensure: The best solution -$\triangle$
1: $g \leftarrow 0$;
2: for $i = 1$ to $M$ do
3:     for $j = 1$ to 3 do
4:         $X_{i,0,j} = X_{\min,j} + rand(0,1) \cdot (X_{\max,j} - X_{\min,j})$
5:     end for
6: end for
7: while $f_t(\triangle) \ge \varepsilon$ and $g \le N$ do
8:     for $i = 1$ to $M$ do
9:         ▶ Basin Hopping
10:        $V_{i,g} = BH(X_{i,g}, I)$
11:        ▶ Crossover
12:        for $j = 1$ to 3 do
13:            $U_{i,g,j} = Crossover(V_{i,g,j}, X_{i,g,j})$
14:        end for
15:        ▶ Selection
16:        if $f_t(U_{i,g}) \le f_t(X_{i,g})$ then
17:            $X_{i,g} = U_{i,g}$
18:            if $f_t(X_{i,g}) \le f_t(\triangle)$ then
19:                $\triangle = X_{i,g}$
20:            end if
21:        else
22:            $X_{i,g} = X_{i,g}$
23:        end if
24:    end for
25:    $g \leftarrow g + 1$
26: end while
```

4 EXPERIMENTAL RESULTS AND ANALYSIS

4.1 Experiment Settings

We conduct experiments based on ImageNet [28]and CASIA-WebFace [37]. In detail, we randomly select 1,000 images from them to conduct the related experiments. We choose six classification models with different structures which are widely used in the literature as threat models: Alexnet [14], VGG19 [32], SqueezeNet[11], Resnet101 [8], InceptionV1 [34] and InceptionV3 [35]. We also compare with other black-box attack methods to verify the proposed method: spatial attack [4], boundary attack [1], single-pixel attack [33] and pointwise attack[29]. As for these attack methods, we adopt their benchmark approaches and default parameters as recommended in Foolbox [27].

Table 1: Selection of hyper-parameters in BHE

	$I = 1$	$I = 2$	$I = 3$	$I = 4$	$I = 5$	$I = 6$	Average
CR=0.5	56.8%	59.3%	58.1%	58.1%	**60.0%**	58.1%	58.4%
CR=0.6	56.2%	56.2%	57.5%	57.5%	59.3%	58.7%	57.6%
CR=0.7	56.8%	58.1%	58.7%	59.3%	59.3%	**60.0%**	58.7%
CR=0.8	56.8%	58.7%	56.8%	**60.0%**	**60.0%**	**60.0%**	58.7%
CR=0.9	58.1%	58.1%	**60.0%**	59.7%	59.3%	59.3%	58.9%
CR=1.0	57.5%	59.3%	59.3%	**60.0%**	**60.0%**	**60.0%**	59.3%
Average	57.0%	58.3%	58.4%	58.9%	59.6%	59.3%	58.6%

Table 2: The attack success rates of individual logo or text watermark.

ACMMM logo watermarks						
	Alexnet	VGG19	SqueezeNet1_0	Resnet101	InceptionV3	Average
scale=2/3	88%/**92%**	77%/**83%**	85%/**88%**	78%/**83%**	77%/**79%**	81%/**85%**
scale=1/2	80%/**88%**	69%/**80%**	76%/**82%**	70%/**78%**	65%/**74%**	72%/**80%**
scale=1/3	68%/**76%**	54%/**68%**	56%/**69%**	56%/**66%**	51%/**61%**	57%/**68%**
scale=1/4	58%/**69%**	43%/**59%**	46%/**62%**	47%/**58%**	41%/**52%**	47%/**60%**
Average	74%/**81%**	61%/**72%**	66%/**75%**	63%/**71%**	59%/**62%**	65%/**73%**
University logo watermarks						
	Alexnet	VGG19	SqueezeNet1_0	Resnet101	InceptionV3	Average
scale=2/3	96%/**98%**	96%/**96%**	95%/**97%**	96%/**97%**	96%/**98%**	96%/**97%**
scale=1/2	90%/**95%**	88%/**90%**	88%/**91%**	88%/**90%**	87%/**91%**	89%/**92%**
scale=1/3	78%/**88%**	74%/**76%**	73%/**79%**	72%/**76%**	68%/**77%**	73%/**79%**
scale=1/4	66%/**78%**	62%/**66%**	61%/**71%**	60%/**66%**	54%/**63%**	61%/**69%**
Average	83%/**90%**	80%/**82%**	80%/**84%**	79%/**82%**	76%/**82%**	80%/**84%**
Text watermarks						
	Alexnet	VGG19	SqueezeNet1_0	Resnet101	InceptionV3	Average
font size=40	89%/**91%**	**82%**/81%	84%/**85%**	74%/**76%**	68%/**73%**	79%/**81%**
font size=36	85%/**89%**	**79%**/78%	80%/**83%**	69%/**73%**	63%/**69%**	75%/**78%**
font size=32	82%/**85%**	75%/**76%**	76%/**80%**	65%/**69%**	58%/**65%**	71%/**75%**
font size=28	75%/**80%**	70%/**71%**	71%/**75%**	59%/**66%**	53%/**60%**	66%/**70%**
Average	83%/**86%**	76%/**76%**	78%/**81%**	67%/**71%**	61%/**66%**	73%/**76%**

Table 3: The attack success rates with limit of embedded watermark position

	scale=1/4	scale=1/5	scale=1/6	scale=1/7	scale=1/8
MIT logo	62%	58%	56%	55%	54%
ACMMM2020	63%	59%	58%	57%	53%
	font size=22	font size=21	font size=20	font size=19	font size=18
Red text	61%	57%	55%	53%	50%

Table 4: Comparison with other attack methods

Network \ attacker	Spatial Attack	Boundary Attack	Single-Pixel	Pointwise Attack	SU logo	ACMMM2017	Blue text
Resnet101	52%	37%	5%	7%	88%	75%	73%
InceptionV3	58%	48%	5%	-	87%	72%	67%

4.2 Optimization method implementation

The initial value of the step size r is set as 0.5. And the initial p, q and α are set as 0, 0 and 100. The range of the p is $[0, W_h - W_{sw}]$. The range of the q is $[0, H_h - H_{sw}]$. And the range of the α is $[100, 200]$.

4.3 Selection of hyper-parameters

We conduct a large number of experiments to determine two hyper parameters in BHE. One is the number of basin hopping iterations I, the other one is crossover probability CR. We adopt BHE to attack DNN models using ACMMM 2020 logo with scale=1/4. In detail, we compute the attack success rates of the Resnet101 on 1000

Table 5: Performance on the state-of-the-art image transformation defense methods

Network	attacker / defender	Single-pixel Attack	Boundary Attack	CMU(1.5/2/3/4)	ACMMM2020(1.5/2/3/4)
Resnet101	Jpeg defend	24%	13%	100%/98%/94%/92%	97%/95%/88%/83%
	Comdefend	17%	13%	99%/94%/88%/82%	97%/94%/89%/82%
	HGD	42%	34%	98%/95%/95%/94%	97%/95%/92%/90%
InceptionV3	Jpeg defend	42%	8%	100%/97%/94%/91%	99%/95%/90%/87%
	Comdefend	34%	12%	99%/95%/91%/86%	98%/94%/90%/86%
	HGD	32%	36%	98%/95%/89%/88%	95%/90%/86%/85%

random image of the ImageNet dataset. The result is shown in Table 1. From Table 1, it is clear that the attack success rate increases when I increases. That is, as the number of Basin Hopping iterations increases, the solution generated by BH will be better, resulting in achieving a higher attack success rate. But more iterations mean more time spent. Considering time complexity, we set CR to 0.9 and I to 3. In this way, Adv-watermark can achieve the highest attack success rate(60%). And in the original BH algorithm, the iteration I is set to 450.

4.4 Attack performance

Six well-trained neural network models which include Alexnet, VGG19, SqueezeNet, Resnet101, InceptionV1 and InceptionV3 are used as threat models. In order to verify the proposed method comprehensively, we choose five university logo watermarks and five official ACMMM watermarks as the image watermarks to generate corresponding adversarial examples. And we also choose five different color fonts as the text watermarks to generate corresponding adversarial examples. The average attack success rates of individual logos or text watermarks are reported in Table 2. The first column of each row shows the results of BH and the second column of each row shows the results of BHE. It is clear that the proposed BHE can achieve a high attack success rate. As for the university logo watermarks, when the watermark size is set as $4/9$ of the host image size, the attack success rate can achieve about 97%. And when the watermark size is set as$1/16$ of the host image size, the attack rate also can achieve 69%. As for the ACMMM logo watermarks, the average attack success rates of them drop a little. That is because that the height-width ratio of the ACMMM watermark is not 1:1(the height-width ratios of the ACMMM logo watermarks(2016-2020) are $1:2.6$, $1:2.5$, $1:3$, $1:2.1$ and $1:2.6$), and the size of the ACMMM logo watermark is smaller than the university logo watermark when the scale is the same. In detail, when scale=$1/4$, the size of ACMMM2018 logo watermark is about $1/48$ of the host watermark size. Even though the performance of the adversarial ACMMM logo watermarks declines a little, they also achieve a high attack success rate. Especially, when the watermark size is $1/48$ of the host image size, the attack success rate can achieve about 50%. Simultaneously, we use the text watermark to attack the well-trained classification models. As shown in Table 2, the proposed method can achieve about 86%, 76%, 81%, 71% and 66% average attack success rates on Alexnet, VGG19, SqueezeNet, Resnet101 and InceptionV3 with different font sizes. Compared with BH, the proposed BHE can achieve a higher attack success rate. Moreover, we conduct a series of experiments on the CASIA-WebFace dataset within restricting adversarial watermark position. Specifically, as shown in Figure 6 (a), we use MTCNN [38] to find face area which is marked as the red rectangle. We restrict the embedded watermark to the area on both sides of the rectangle which is marked as the green rectangle. And then we use Adv-watermark to attack InceptionV1 which is trained on CASIA-WebFace dataset. Generated adversarial examples are shown in Figure 6 (b). The attack result is shown in Table 3. Note that since we limit the embedding area of the watermark, we should adopt a smaller scale and font size. It is clear that even if we limit the area of attack, the proposed attack method can also achieve excellent performance.

Table 6: Performance on the adversarial training

Adversarial Training	MIT		ACMMM20		Red Text	
	1/4	1/3	1/4	1/3	28	32
MIT(1/4)	**50%**	**55%**	74%	80%	91%	92%
ACMMM20(1/4)	78%	83%	**43%**	**48%**	85%	86%
Red Text(28)	71%	74%	72%	86%	**44%**	**47%**

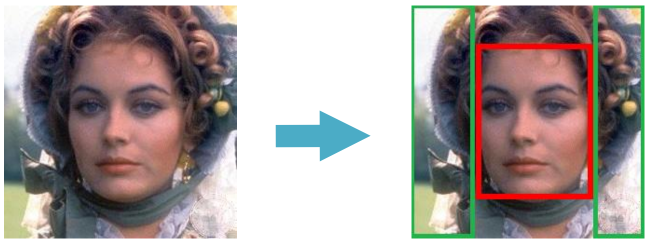

(a) Position of Embedded Watermark

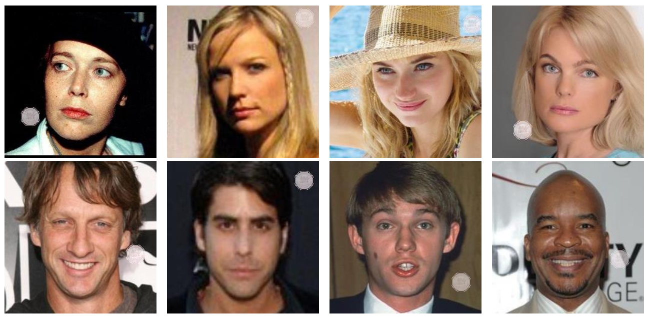

(b) Adversarial Examples

Figure 6: (a) Limit of embedded watermark position. The face is in the red rectangle and the embedded watermark is restricted to the green rectangles. (b) Adversarial examples on the CASIA-WebFace dataset.

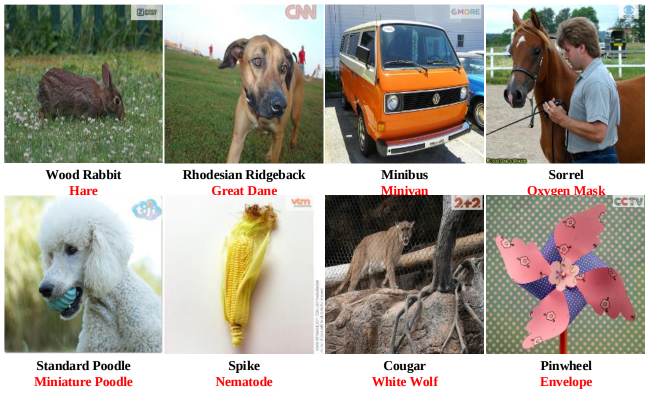

Figure 7: The adversarial examples with a variety of TV station logos. The original class labels are in black color and the class labels of the adversarial examples are in red color.

4.5 Comparisons with other attack methods

To quantitatively evaluate the proposed method performance, we compare the proposed method with other black-box attack methods: spatial attack [4], boundary attack [1], single-pixel attack [33] and pointwise attack[29]. In detail, we choose the SU and ACMMM2017 image watermarks with different scales and blue font text watermark with the different font sizes to complete the contrast experiments. Their average attack success rates are shown in Table 4. As shown in Table 4, it is clear that compared with other black-box attack methods, our attack method can achieve a higher attack success rate. In particular, the average attack success rate of SU reaches up to 88%.

In order to evaluate the robustness of the proposed method, we compare the Adv-watermark with other black-box attack methods: single-pixel attack and boundary attack, and choose three image transformation defense methods: Jpeg defend [3], Comdefend [12] and HGD [17]. We use the attack methods to attack the Resnet101 and InceptionV3 to generate corresponding adversarial examples, next apply three defend methods to defend the adversarial examples and then count their respective attack success rates. From Table 5, it is clear that the existing image transformation defense methods are useful for single-pixel attack and boundary attack, but not useful for our proposed method. Compared with other attack methods, the proposed method is more robust. We also conduct adversarial training [19] to defend the proposed attack method. In detail, we inject adversarial examples generated by MIT, ACMMM2020 image watermark with scale = 1/4 and red text watermark with font = 28 into the original image dataset and retrain three Resnet101 on them respectively. And then we use these watermarks with different sizes to attack these models. The result is shown in Table 6. It is clear that the adversarial training cannot effectively defend Adv-watermark. Moreover, using another watermark to attack the adversarial training model can achieve a higher attack success rate. In other words, even though adversarial training increases the robustness to one watermark perturbation, it increases the vulnerability to another watermark perturbation.

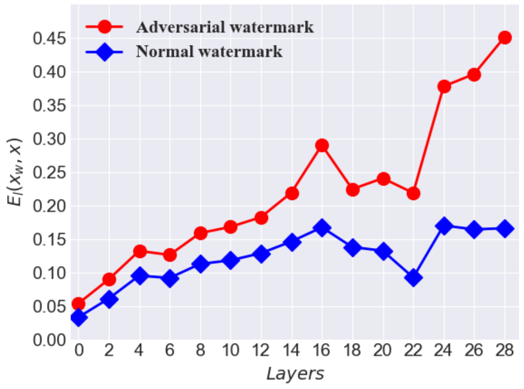

Figure 8: Layer-wise perturbation levels of the VGG16 model. Adversarial watermark and normal watermark added to clean images correspond to the E_l, respectively.

4.6 Extension

The proposed method is not limited to using a watermark to generate an adversarial example. It can be extended to use the TV station logos to complete the attack. To make the generated adversarial examples more realistic and imperceptible, we also choose more commonly used TV station logos to complete the attack. In detail, we select a variety of TV station logos, next limit the embedded position of the logos to the upper right corner of the host image and then use the proposed method to generate the adversarial examples. As shown in Figure 7, the generated adversarial examples are more realistic and common in the physical world.

4.7 Analysis for Adv-watermark

Compared with the previous attack methods, Adv-watermark pays more attention to generate realistic adversarial examples. We find DNN models are spatially vulnerable, which adding perturbations at a specific position to clean images can attack them easily. This makes it possible to attack DNN models by using watermarks. In detail, DNN models can be attacked by adding specific transparency watermarks to a specific position in clean images. To investigate this characteristic, we conduct a comparative experiment to evaluate layer-wise perturbations of the VGG16 model fed adversarial watermark images and normal watermark images, respectively. The difference between normal watermarks and adversarial watermarks is that they are positioned differently on clean images. The perturbation level in layer l can be formulated as:

$$E_l\left(x_w, x\right) = \left\|f_l\left(x_w\right) - f_l(x)\right\|_2 / \left\|f_l(x)\right\|_2 , \qquad (12)$$

where x represents a clean image, x_w represents the clean image with adversarial or normal watermark and $f_l(\cdot)$ represents the l-th layer of the VGG16 model.

The result is shown in Figure 8. The red curve represents the E_l for adversarial watermark perturbations and the blue curve represents the E_l for normal watermark perturbations. Specifically, the red curve is the average result on 30 randomly picked images with the adversarial watermarks and the blue curve is the average result on 30 same images with the normal watermarks. It is clear that the watermark perturbation is progressively enlarged with the layer hierarchy. But in the top layer, the adversarial watermark perturbation is much higher than the normal watermark perturbation. Because the classification result is dependent on the top-level features, the adversarial watermark perturbation can fool DNN models but the normal watermark perturbation can not. Moreover we find that the pooling layer not only can remove the redundant image information but also can reduce the impact of the watermark perturbation. But for the adversarial watermark perturbation, the pooling layer does not effectively reduce its impact. Note that even though the adversarial watermark is not added to the recognized object, it can also attack the DNN models successfully. Please refer to Figure 7.

5 CONCLUSION

In this paper, we discovered DNN models were spatially vulnerable, which adding perturbations at a specific position to clean images could attack models easily. And then we proposed a novel attacking method which used the real watermark to attack the well-trained classifier. Our adversarial perturbation was meaningful, which was different from the traditional ones. We formulated the watermark attack problem as a global optimization problem, and proposed a novel optimization algorithm(BHE) to generate adversarial examples. Compared with the previous BH, BHE achieved a higher attack success rate and was more efficient. In detail, generating an adversarial example only needed to query the well-trained classification model less than 1000 times. Moreover, the Adv-watermark was more robust, because the state-of-the-art image transformation defense methods could not defend the adversarial examples generated by the proposed method. And the proposed method could be more commonly used in the real world.

REFERENCES

[1] Wieland Brendel, Jonas Rauber, and Matthias Bethge. 2017. Decision-Based Adversarial Attacks: Reliable Attacks Against Black-Box Machine Learning Models. arXiv:1712.04248 [stat.ML]

[2] Nicholas Carlini and David Wagner. 2017. Towards evaluating the robustness of neural networks. In *2017 IEEE Symposium on Security and Privacy (SP)*. IEEE, 39–57.

[3] Nilaksh Das, Madhuri Shanbhogue, Shang-Tse Chen, Fred Hohman, Li Chen, Michael E Kounavis, and Duen Horng Chau. 2017. Keeping the bad guys out: Protecting and vaccinating deep learning with jpeg compression. *arXiv preprint arXiv:1705.02900* (2017).

[4] Logan Engstrom, Brandon Tran, Dimitris Tsipras, Ludwig Schmidt, and Aleksander Madry. 2019. Exploring the Landscape of Spatial Robustness. In *International Conference on Machine Learning*. 1802–1811.

[5] Ian Goodfellow, Jean Pouget-Abadie, Mehdi Mirza, Bing Xu, David Warde-Farley, Sherjil Ozair, Aaron Courville, and Yoshua Bengio. 2014. Generative adversarial nets. In *Advances in neural information processing systems*. 2672–2680.

[6] Ian J Goodfellow, Jonathon Shlens, and Christian Szegedy. 2014. Explaining and harnessing adversarial examples. *arXiv preprint arXiv:1412.6572* (2014).

[7] Frank Hartung and Martin Kutter. 1999. Multimedia watermarking techniques. *Proc. IEEE* 87, 7 (1999), 1079–1107.

[8] Kaiming He, Xiangyu Zhang, Shaoqing Ren, and Jian Sun. 2016. Deep residual learning for image recognition. In *Proceedings of the IEEE conference on computer vision and pattern recognition*. 770–778.

[9] Yongjian Hu, Sam Kwong, and Jiwu Huang. 2005. An algorithm for removable visible watermarking. *IEEE Transactions on Circuits and Systems for Video Technology* 16, 1 (2005), 129–133.

[10] Biao-Bing Huang and Shao-Xian Tang. 2006. A contrast-sensitive visible watermarking scheme. *IEEE MultiMedia* 13, 2 (2006), 60–66.

[11] Forrest N Iandola, Song Han, Matthew W Moskewicz, Khalid Ashraf, William J Dally, and Kurt Keutzer. 2016. SqueezeNet: AlexNet-level accuracy with 50x fewer parameters and< 0.5 MB model size. *arXiv preprint arXiv:1602.07360* (2016).

[12] Xiaojun Jia, Xingxing Wei, Xiaochun Cao, and Hassan Foroosh. 2019. ComDefend: An Efficient Image Compression Model to Defend Adversarial Examples. In *Proceedings of the IEEE Conference on Computer Vision and Pattern Recognition*. 6084–6092.

[13] Mohan S Kankanhalli, KR Ramakrishnan, et al. 1999. Adaptive visible watermarking of images. In *Proceedings IEEE International Conference on Multimedia Computing and Systems*, Vol. 1. IEEE, 568–573.

[14] Alex Krizhevsky, Ilya Sutskever, and Geoffrey E Hinton. 2012. Imagenet classification with deep convolutional neural networks. In *Advances in neural information processing systems*. 1097–1105.

[15] Alexey Kurakin, Ian Goodfellow, and Samy Bengio. 2016. Adversarial examples in the physical world. *arXiv preprint arXiv:1607.02533* (2016).

[16] Ares Lagae, Sylvain Lefebvre, Rob Cook, Tony DeRose, George Drettakis, David S Ebert, John P Lewis, Ken Perlin, and Matthias Zwicker. 2010. A survey of procedural noise functions. In *Computer Graphics Forum*, Vol. 29. Wiley Online Library, 2579–2600.

[17] Fangzhou Liao, Ming Liang, Yinpeng Dong, Tianyu Pang, Xiaolin Hu, and Jun Zhu. 2018. Defense against adversarial attacks using high-level representation guided denoiser. In *Proceedings of the IEEE Conference on Computer Vision and Pattern Recognition*. 1778–1787.

[18] Tsung-Yuan Liu and Wen-Hsiang Tsai. 2010. Generic lossless visible watermarkingâĂŤa new approach. *IEEE transactions on image processing* 19, 5 (2010), 1224–1235.

[19] Aleksander Madry, Aleksandar Makelov, Ludwig Schmidt, Dimitris Tsipras, and Adrian Vladu. 2018. Towards Deep Learning Models Resistant to Adversarial Attacks. In *ICLR (Poster)*. OpenReview.net.

[20] Fred Mintzer, Gordon W Braudaway, and Minerva M Yeung. 1997. Effective and ineffective digital watermarks. In *Proceedings of International Conference on Image Processing*, Vol. 3. IEEE, 9–12.

[21] Frederick C Mintzer, Leonard E Boyle, Albert N Cazes, Brian S Christian, Steven C Cox, Francis P Giordano, Henry M Gladney, Jack C Lee, Milton L Kelmanson, Antonio C Lirani, et al. 1996. Toward on-line, worldwide access to Vatican Library materials. *IBM Journal of research and development* 40, 2 (1996), 139–162.

[22] Seyed-Mohsen Moosavi-Dezfooli, Alhussein Fawzi, Omar Fawzi, and Pascal Frossard. 2017. Universal adversarial perturbations. In *Proceedings of the IEEE conference on computer vision and pattern recognition*. 1765–1773.

[23] Seyed-Mohsen Moosavi-Dezfooli, Alhussein Fawzi, and Pascal Frossard. 2016. Deepfool: a simple and accurate method to fool deep neural networks. In *Proceedings of the IEEE conference on computer vision and pattern recognition*. 2574–2582.

[24] Nicolas Papernot, Patrick McDaniel, Somesh Jha, Matt Fredrikson, Z Berkay Celik, and Ananthram Swami. 2016. The limitations of deep learning in adversarial settings. In *2016 IEEE European Symposium on Security and Privacy (EuroS&P)*. IEEE, 372–387.

[25] Nicolas Papernot, Patrick McDaniel, Xi Wu, Somesh Jha, and Ananthram Swami. 2016. Distillation as a defense to adversarial perturbations against deep neural networks. In *2016 IEEE Symposium on Security and Privacy (SP)*. IEEE, 582–597.

[26] Haonan Qiu, Chaowei Xiao, Lei Yang, Xinchen Yan, Honglak Lee, and Bo Li. 2019. SemanticAdv: Generating Adversarial Examples via Attribute-conditional Image Editing. *arXiv preprint arXiv:1906.07927* (2019).

[27] Jonas Rauber, Wieland Brendel, and Matthias Bethge. 2017. Foolbox: A Python toolbox to benchmark the robustness of machine learning models. In *Reliable Machine Learning in the Wild Workshop, 34th International Conference on Machine Learning*. http://arxiv.org/abs/1707.04131

[28] Olga Russakovsky, Jia Deng, Hao Su, Jonathan Krause, Sanjeev Satheesh, Sean Ma, Zhiheng Huang, Andrej Karpathy, Aditya Khosla, Michael Bernstein, et al. 2015. Imagenet large scale visual recognition challenge. *International journal of computer vision* 115, 3 (2015), 211–252.

[29] Lukas Schott, Jonas Rauber, Matthias Bethge, and Wieland Brendel. 2018. Towards the first adversarially robust neural network model on MNIST. arXiv:1805.09190 [cs.CV]

[30] Ramprasaath R. Selvaraju, Michael Cogswell, Abhishek Das, Ramakrishna Vedantam, Devi Parikh, and Dhruv Batra. 2017. Grad-CAM: Visual Explanations From Deep Networks via Gradient-Based Localization. In *The IEEE International Conference on Computer Vision (ICCV)*.

[31] Bo Shen, Ishwar K Sethi, and Vasudev Bhaskaran. 1998. DCT domain alpha blending. In *Proceedings 1998 International Conference on Image Processing. ICIP98 (Cat. No. 98CB36269)*, Vol. 1. IEEE, 857–861.

[32] Karen Simonyan and Andrew Zisserman. 2014. Very deep convolutional networks for large-scale image recognition. *arXiv preprint arXiv:1409.1556* (2014).

[33] Jiawei Su, Danilo Vasconcellos Vargas, and Kouichi Sakurai. 2019. One pixel attack for fooling deep neural networks. *IEEE Transactions on Evolutionary Computation* (2019).

[34] Christian Szegedy, Wei Liu, Yangqing Jia, Pierre Sermanet, Scott E. Reed, Dragomir Anguelov, Dumitru Erhan, Vincent Vanhoucke, and Andrew Rabinovich. 2015. Going deeper with convolutions. In *CVPR*. IEEE Computer Society, 1–9.

[35] Christian Szegedy, Vincent Vanhoucke, Sergey Ioffe, Jon Shlens, and Zbigniew Wojna. 2016. Rethinking the inception architecture for computer vision. In *Proceedings of the IEEE conference on computer vision and pattern recognition*.

2818–2826.

[36] David J Wales and Jonathan P K Doye. 1997. Global Optimization by Basin-Hopping and the Lowest Energy Structures of Lennard-Jones Clusters Containing up to 110 Atoms. *Journal of Physical Chemistry A* 101, 28 (1997), 5111–5116.

[37] Dong Yi, Zhen Lei, Shengcai Liao, and Stan Z Li. 2014. Learning face representation from scratch. *arXiv preprint arXiv:1411.7923* (2014).

[38] Kaipeng Zhang, Zhanpeng Zhang, Zhifeng Li, and Yu Qiao. 2016. Joint Face Detection and Alignment Using Multitask Cascaded Convolutional Networks. *IEEE Signal Process. Lett.* 23, 10 (2016), 1499–1503.